Time-Hopped Ultrawide Bandwidth Receiver Designs Using Multiuser Interference Sensing

David J. Young and Norman C. Beaulieu
*i*CORE Wireless Communications Laboratory
Edmonton, Alberta, Canada T6G 2V4
{djyoung,beaulieu}@ece.ualberta.ca

***Abstract*—The uncoordinated nature of impulse radio ultra-wide bandwidth (UWB) transmissions leads to multiple-user interference (MUI) at each receiver. Due to use of a repetition code and multipath propagation, a Rake receiver has many partial decision statistics available for use in forming a symbol decision. Novel time-hopped UWB Rake receiver structures have been designed that aim to mitigate MUI by sensing the presence of MUI in the partial decision statistics associated with each received symbol. The presented IS method responds to mistimed pulses arising from interfering users for each repeated pulse (frame) of the symbol, in each Rake finger, yielding a signal that is correlated with signals from interfering users but uncorrelated with the desired-user signal. Receivers are presented that use MUI-sensing in selection of the best received pulses for combining, i.e., pulses less likely to be catastrophically corrupted by a pulse due to an interfering user. Also considered are nonlinear receiver structures in which MUI-sensing is used to select a subset of partial decision statistics to undergo nonlinear processing and/or combining.**

I. Introduction

Ultra-wide bandwidth (UWB) systems are an attractive technique for simultaneous, collocated frequency reuse, making available a wide bandwidth for unlicensed applications. This bandwidth might otherwise go unused at a particular time and point in space, but extremely low transmitted power spectral density allows UWB systems to underlay licensed narrowband users without causing harmful interference.

Impulse radio (IR) UWB systems use an ultra-short signaling pulse transmitted at baseband. Indoor UWB applications suggest a number of similar devices may be located at close range, and the uncoordinated nature of IR-UWB transmissions from different users leads to multiple-user interference (MUI) at each receiver. Use of a time-hopping (TH) code together with a low duty cycle provides some protection against catastrophic interference from multiple users, imparting each transmitted pulse in a symbol with a time shift according to a code unique to each user[1], [2]. However, a conventional matched-filter (CMF) receiver has been shown to be ineffective in the presence of significant MUI, and in particular does not efficiently exploit the potential of the time-hopping system.

Time-hopped systems have substantially different MUI characteristics than IR-UWB systems that employ direct-sequence codes, or multiband UWB systems, and demand different MUI models for use in system analysis and design; the Gaussian interference model which has been used extensively for a variety of communication systems is generally not an accurate model for this case. The problem of MUI in TH-UWB communication systems has been examined in a number of published works (see [3] and references therein). Many of the receiver structures considered in these works treat MUI due to interfering impulse radios as an additional source of (non-Gaussian) noise at the receiver. The MUI is characterized by probability distributions with heavier tails than the Gaussian distribution, more suitable for modeling impulsive disturbances. For example, the Laplace distribution[4], [5], generalized Gaussian distribution[6], and alpha-stable distribution[7] have been considered for modeling MUI or MUI-plus-AWGN. Receivers are designed according to each MUI model. Since an effective UWB receiver must work well in the continuum between the low-SNR–high-SIR regime, which will have Gaussian noise as a dominant impairment, and the high-SNR–low-SIR regime, which will be dominated by non-Gaussian interference, the best receivers have adaptive implementations[3].

The present work takes a different approach. The repetition code and multipath channel provide rich diversity at the receiver, and the new approach takes advantage of the TH-UWB signaling format to develop interference-sensing (IS) statistics useful in processing and combining the received pulses for each symbol. TH-UWB symbols are typically transmitted over many frames, with one pulse per frame, and the use of time-hopping implies that relatively few of the transmitted pulses associated with a given source symbol are likely to overlap pulses from a different user with a different hopping code; some frames will experience catastrophic interference but others will experience little to no interference. This motivates structures which sense interference on a frame-by-frame basis without relying on a stochastic interference model. The IS signal can be used to select some frames for inclusion in the decision statistic for a particular symbol, and exclude others. The signal can also be used to alter receiver processing on a frame-by-frame basis.

Other work has considered the problem of combining statistics from frames and multipath components (e.g., [8]). Our approach is different, yielding simple structures applicable to both linear and nonlinear receivers.

This paper is structured as follows. Section II provides an overview and the system model. Section III presents one type of MUI-sensing structure. Section IV applies this structure to two forms of IS-based receiver. Performance results and discussion are provided in Section V, and conclusions can be found in Section VI.

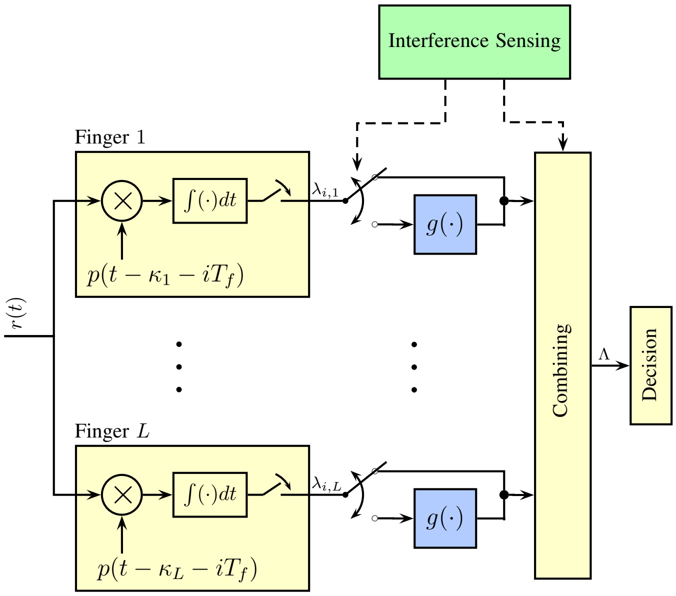

Fig. 1. Generic block diagram of the proposed receiver structures with correlator-level interference sensing. The combining block represents both finger and frame combining.

II. Overview and System Model

The TH-UWB signal format considered here is as follows. Each binary source symbol $d_j^{(k)} \in \{-1, 1\}$ is transmitted over N_s frames of length T_f, with one pulse $p(t)$ of duration $T_p \ll T_f$ per frame. The frames are divided into chip slots of duration T_c, with the slot used to transmit a particular pulse chosen in each frame according to a hopping code $\{c_i^{(k)}\}$ unique to the kth user. With energy per bit E_b, the transmitted TH-BPSK signal for the kth user can be written as

$$s^{(k)}(t) = \sqrt{\frac{E_b}{N_s}} \sum_{i=-\infty}^{\infty} d^{(k)}_{\lfloor i/N_s \rfloor} p\left(t - iT_f - c_i^{(k)} T_c\right) \qquad (1)$$

where $\lfloor x \rfloor$ is the nearest integer less than or equal to x.

An effective TH-UWB receiver must be designed to operate in the dense multipath which characterizes the UWB indoor propagation channel[9], [10]. The basic receiver structure we will consider is the Rake receiver pictured in Fig. 1. (The conventional Rake receiver does not contain the block labeled interference sensing, nor the blocks labeled "$g(\cdot)$"; these will be discussed in the sequel.) Each finger of the Rake receiver is matched to the signal received on a resolvable path or group of paths, and correlates the received signal with a template pulse at relative delay κ_l. The fine time resolution of impulse radio UWB signals leads to a large number of resolvable paths, and an impractically large number of Rake fingers may be needed to capture all signal energy. The receivers considered here are selection Rake receivers, which match a reduced number of Rake fingers, L, to the strongest received paths. The signal amplitude on the lth path will be denoted α_l.

The combining block in Fig. 1 produces a weighted sum of the L finger outputs for all N_s frames used to transmit a given source symbol. Each of the $N_s L$ finger outputs $\lambda_{i,l}$ will be termed a partial decision statistic (PDS). The receivers we will consider use maximal-ratio combining (MRC) of correlator PDSs from L fingers to form N_s frame PDSs, and equal-gain combining of frame PDSs to form the overall decision statistic. The receiver decides on the transmitted symbol based on the sign of the decision statistic Λ.

The conventional receiver using linear combining is the optimal receiver when the only channel impairment is AWGN, but it does not perform well in the presence of significant MUI which is non-Gaussian[3]. Accurate characterizations for the probability distribution of the MUI lead to a receiver designs with an appropriate nonlinear $g(\cdot)$ block in each finger, applied to each correlator PDS (i.e., in Fig. 1, all switches are set to the lower position).

The receivers proposed in this paper introduce the interference sensing block pictured in Fig. 1. The purpose of this block is to indicate, on a per-PDS basis, which frames may have experienced catastrophic overlap with a pulse from a different user. Observing Fig. 2, a collision has occurred in the pictured frame, but in a subsequent frame likely the pulses will hop to non-overlapping chip slots. Moreover, in the noise-free simplified example of Fig. 2, the low duty cycle suggests that it is possible to detect pulse collisions by the presence of signal energy just outside the user 1 correlation window. Noise and multipath complicates the pictured model, but it can be shown[11] that correlation with the user 1 pulse does not form a sufficient statistic for detection in the presence of MUI, and thus a MUI-sensing statistic may be useful.

III. An MUI-Sensing Correlator Structure

The received signal for the user of interest consists of a superposition of the desired-user transmitted signal (after channel propagation effects), AWGN, and interfering user signals (after different channel propagation effects). When all interfering users employ a common signaling pulse shape, the interference process will itself be a superposition of pulses of common shape. The pulses due to the other users are time-shifted since users transmit asynchronously and according to their own time-hopping code, scaled due to propagation effects such as path length, and possibly inverted by interferer data bits. Superposition of pulses is also due to multipath propagation, with each propagation path having an associated delay, attenuation, and possible inversion. Each pulse transmitted by every user gives rise to a large number of pulses at the receiver.

We therefore form an IS signal that responds to this common pulse shape when a received pulse is time-shifted from the desired pulse, but that does not respond to a pulse at the correct timing.[1]

[1] An interfering pulse which is essentially in synchronism with the desired pulse will occur with some nonzero probability. The proposed IS schemes instead detect shifted (mistimed) pulses, which can have significant destructive effect on the PDS, and which have higher probability of occurrence than a perfectly-timed interfering pulse. Use of the PDS and IS together for PDS selection is accomplished by an IS-zonal structure considered in [11] following from the work of [12]. IS receivers using nonlinear PDS transformations can also be viewed as an IS-PDS approach to MUI mitigation.

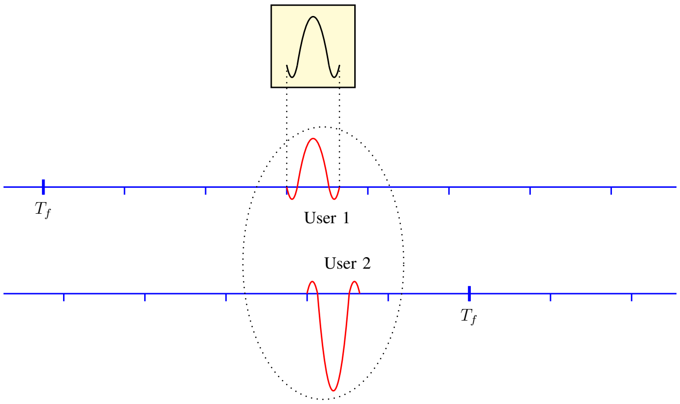

Fig. 2. An example TH-UWB pulse in the absence of noise and interference, together with an asynchronous TH-UWB interfering pulse. The box indicates the typical user-1 correlation template.

Let a single received desired-user pulse $p(t)$, $0 \leq t \leq T_p$ be sampled at rate $1/T_q$ to form a vector of N_q samples, $\mathbf{p} = [p(0), p(T_q), \ldots, p((N_q-1)T_q)]^\top \equiv [[p(nT_q)]]_{n=0}^{N_q-1}$. Note that $p(t)$ has been time-shifted to the origin and is normalized to unit energy. The received signal $r(t)$ is sampled at the same instants to form vector $\mathbf{r} = [[r(nT_q)]]_{n=0}^{N_q-1}$ and correlated in discrete time with a length-N_q template $\mathbf{v}$. The AWGN component of the sampled received signal is denoted $\mathbf{z}$, while the normalized component of $\mathbf{r}$ due to the kth interfering user in the ith frame is denoted $\mathbf{p}_{\theta_i^{(k)}} = [[p(nT_q - \theta_i^{(k)})]]_{n=0}^{N_q-1}$. The ith partial decision statistic can therefore be written

$$\lambda_i = \mathbf{r}^\top \mathbf{v} = A_c d \mathbf{p}^\top \mathbf{v} + \sum_k A_k d_k \mathbf{p}_{\theta_i^{(k)}}^\top \mathbf{v} + \mathbf{z}_i^\top \mathbf{v} \tag{2}$$

where d and A_c are the data symbol and chip amplitude of the desired user, respectively, and A_k and d_k are the data symbol and chip amplitude of the kth interfering user.

The IS structure considered here is termed an IS correlator, and forms

$$\xi_i = \mathbf{r}^\top \mathbf{u} = A_c d \mathbf{p}^\top \mathbf{u} + \sum_k A_k d_k \mathbf{p}_{\theta_i^{(k)}}^\top \mathbf{u} + \mathbf{z}_i^\top \mathbf{u}. \tag{3}$$

Ideally, ξ_i contains no contribution from the first term of (3); i.e., $\mathbf{u}$ and $\mathbf{p}$ are orthogonal so $\mathbf{p}_0^\top \mathbf{u} = 0$. Also, the second term of (3) should be representative of the second term of (2); ideally, $\mathbf{p}_{\theta_i^{(k)}}^\top \mathbf{u} = \mathbf{p}_{\theta_i^{(k)}}^\top \mathbf{v}$ for $\theta_i^{(k)} \neq 0$.

The various sources of time offset for each interferer have been summarized in the single random variable $\theta_i^{(k)}$. The hopping code ensures each frame has a unique realization of $\{\theta_i^{(k)}\}$, $\{A_k\}$, and $\{d_k\}$, making an exact frame-dependent solution for $\mathbf{u}$ impractical. Instead, a set of uniformly spaced $\{\theta_i^{(k)}\}$ will be used to determine a static template $\mathbf{u}$ that does not depend on the particular interferer realization, but does respond to typical MUI realizations.

The resulting system of linear equations is, in matrix form,

$$\mathbf{W}\mathbf{P}_S \mathbf{u} = \mathbf{W}\mathbf{d}_S. \tag{4}$$

The N_qth row of (4) corresponds to the desired-user signal, while each remaining row corresponds to a test $\mathbf{p}_{\theta_i^{(k)}}$, i.e., a shifted pulse due to an interferer. The ith column of the $(2N_q - 1) \times N_q$ matrix $\mathbf{P}_S$ is thus $[\mathbf{0}_{N_q - i}\, \mathbf{p}\, \mathbf{0}_{i-1}]^\top$, where $\mathbf{0}_n$ denotes a length-n vector of zeros, and $i = 1, \ldots, N_q$. The vector $\mathbf{d}_s$ is the desired response vector, equal to zero for the N_qth row, and $\bar{d}_i \mathbf{p}_{\theta_i}^\top \mathbf{v}$ elsewhere, where $\mathbf{p}_{\theta_i}^\top$ is the ith row of $\mathbf{P}_S$ and the $\{\bar{d}_i\}$ are design parameters which control the symmetry of the solution $\mathbf{u}$. A $(2N_q - 1) \times (2N_q - 1)$ diagonal matrix $\mathbf{W}$ can be used to control the optimization via nonnegative weights on its diagonal.

Eqn. (4) is an overdetermined system of $(2N_q - 1)$ equations in N_q unknowns, and generally an exact solution does not exist; the basic construction is ill-posed. To provide an approximate solution while controlling the noise energy in the IS correlator output, the problem can be considered as a Tikhonov regularization problem[13] that seeks to minimize $\|\mathbf{W}(\mathbf{P}_S \mathbf{u} - \mathbf{d}_S)\|^2 + \delta_T \|\mathbf{u}\|^2$ where δ_T is the regularization parameter. Lower δ_T improves the interference-sensing properties of $\mathbf{u}$ in the absence of noise, while higher δ_T gives lower AWGN power in the IS statistic. A typical value for fixed δ_T is $1/2T_q$, or alternately in a given optimization a value for δ_T constraining $\|\mathbf{u}\|^2$ to a particular value can be found.

The problem has analytical solution

$$\mathbf{u} = \left(\mathbf{P}_S^\top \mathbf{W}^2 \mathbf{P}_S + \delta_T \mathbf{I}\right)^{-1} \mathbf{P_S}^\top \mathbf{W}^2 \mathbf{d}_S. \tag{5}$$

The matrix inversion in (5) is always well-conditioned for $\delta_T > 0$. In the case where an assumed pulse shape is used as a receiver template, (5) can be precomputed based on this pulse shape. When the desired-user pulse shape is instead estimated at the receiver, the estimated $\hat{\mathbf{p}}$ can be used in (5) during the receiver set-up phase. Since $\{\bar{d}_i\}$ with odd symmetry and $\{\bar{d}_i\}$ with even symmetry lead to weakly correlated solution templates, both solutions can be used together in one receiver to improve sensitivity to MUI, as in Section V. In the case of the even-symmetric solution, it is necessary to put additional weight on the N_qth row of (4) to effectively null the desired user; this is not needed in the odd-symmetric case.

The correlator response to interfering pulses at various shifts is pictured in Fig. 3 using the second-order Gaussian monocycle pulse $p(t) = (4/\sqrt{6T_m}) \exp[-2\pi(t/T_m)^2][1 - 4\pi(t/T_m)^2]$.

IV. Receiver Structures Employing IS

This section describes receivers in which the processing of each PDS is altered by a hard decision based on each IS statistic (ISS). Two techniques are considered. The first omits a PDS from combining when the magnitude of the corresponding ISS exceeds a threshold. Thus, PDSs are selected for combining based on the ISSs, and this will be termed the "selection" method. In Fig. 1, this is represented by the control of the combiner block by the IS block. The second technique applies a nonlinear operation to each PDS for which the magnitude of the corresponding ISS exceeds a threshold. Other PDSs are passed to the combiner unaltered. We term this the "switching" method. In Fig. 1 this is represented by control of the switches preceding each $g(\cdot)$ block by the IS block.

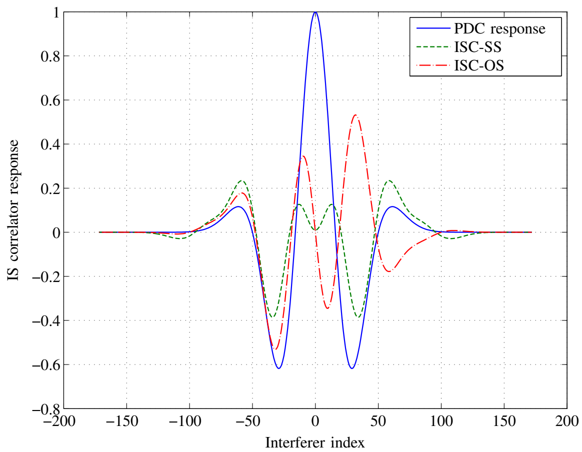

Fig. 3. The interference-sensing correlator response to an interfering pulse, using same-symmetry (ISC-SS) and opposite-symmetry (ISC-OS) interference-sensing correlation templates. The interferer index represents the relative delay of the interfering pulse.

Define a set $\mathcal{J}$ which contains the frame and finger indices (i, l) for IS statistics with magnitude less than a threshold η

$$\mathcal{J} = \{(i, l) | \, |\xi_{i,l}| < \eta\}. \tag{6}$$

Note that the form of (6) is the same for the various receivers considered here, but η is receiver-dependent. The decision statistic for the ISS selection-based receivers can then be written as

$$\Lambda = \sum_{i,l \in \mathcal{J}} \alpha_l g\left(\lambda_{i,l}\right) \tag{7}$$

where $g(x)$ is a PDS transformation function according to the type of receiver. For the linear receiver using MRC weights on each PDS, $g(x) = x$. For the hard-limiting receiver considered here, $g(x) = g_{\text{HL}}(x) = \text{sgn}(x)$. For the soft-limiting receiver

$$g(x) = g_{\text{SL}}(x) = \begin{cases} A_c, & A_c\alpha_l \leq x \\ x/\alpha_l, & -A_c\alpha_l < x < A_c\alpha_l \\ -A_c, & x \leq -A_c\alpha_l. \end{cases} \tag{8}$$

In the block diagram of Fig. 1, the $g(\cdot)$ blocks are always active for the nonlinear selection methods, and IS controls the combiner. Other transformations can also be used, such as the p-order metric transformation of [6] or the zonal-based transformation of [12].

For the switching method, the receiver decision statistic can be written

$$\Lambda = K \sum_{i,l \in \mathcal{J}} \alpha_l g\left(\lambda_{i,l}\right) + \sum_{i,l \notin \mathcal{J}} \alpha_l \lambda_{i,l}. \tag{9}$$

The factor K balances the contributions of the transformed and untransformed PDSs. Within each group, the PDSs should be combined optimally in order that the switching does not cause performance degradation. However, when both forms are present in same overall decision statistic, the relative weighting of the two types of PDS will determine whether ISS-based switching is beneficial. It has been found that $K = 4\sigma_z^{-1}$ gives good performance in the case of a hard or soft limiting nonlinearity.

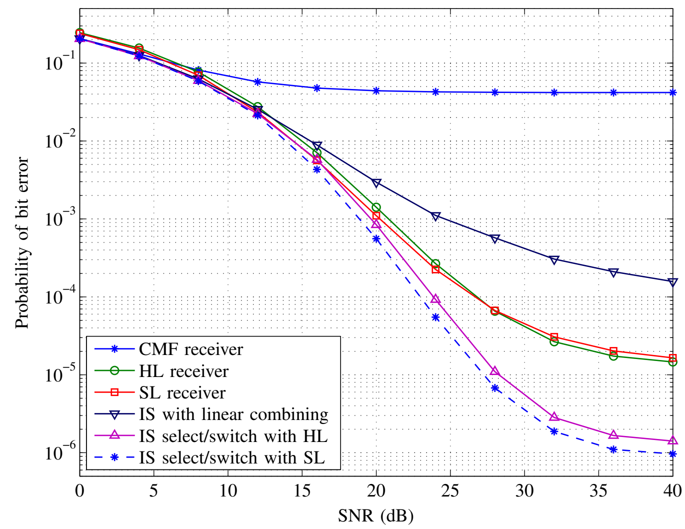

Fig. 4. A comparison of the bit error rate performances of receivers using IS-based selection and switching, as a function of SNR at an average SIR of 8 dB, together with the performances of the corresponding non-IS receivers, for three interfering users in a CM1 multipath channel.

The switching technique closely approaches the performance of the conventional receiver in small SNR or large SIR regions, and closely approaches the performance of the underlying nonlinear receiver in large SNR or small SIR regions. The benefit of switching was observed in the region where both SNR and SIR are moderate. On the other hand, the nonlinear IS-selection receivers are superior in regions of small SIR or large SNR. Therefore, a sensible strategy is to alter the receiver operation based on the average SNR and SIR, with IS used to determine whether the PDS is passed to the combiner as-is, a nonlinear operation is applied to the PDS before combining, or the PDS is omitted from combining. The required IS hardware is the same in each operating mode. Additionally, since fewer PDSs undergo the nonlinear transformation, fewer of these expensive operations are required, offsetting somewhat the extra effort of IS.

V. Performance Results and Discussion

The performances of the various receivers have been evaluated by simulation. Example bit error rate (BER) performance results are presented in Fig. 4 as a function of SNR at an SIR of 8 dB, and in Fig. 5 as a function of SIR at an SNR of 16 dB, with three interfering users of uniform average power. The presented results are for a length-9 selection Rake receiver, operating in an IEEE 802.15.3a CM1 multipath channel[10]. The Rake templates are assumed to be perfectly estimated, and the IS-based receivers form an IS signal for each PDS using a pair of interference-sensing correlators as described in Section III. A second-order Gaussian monocycle pulse shape is used, with 16 frames per symbol, frame duration 160 ns and chip duration 0.9 ns. The threshold η giving the smallest BER has been used for the presented results. The receivers are not overly sensitive to the value of η, and η can be expressed as receiver-dependent functions of average SIR and SNR with negligible loss in performance[11].

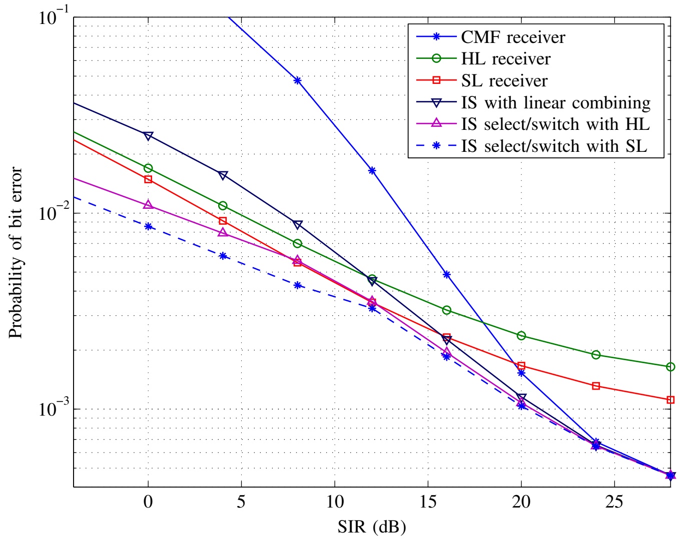

Fig. 5. A comparison of the bit error rate performances of receivers using IS-based selection and switching, as a function of SIR at an average SNR of 16 dB, together with the performances of the corresponding non-IS receivers, for three interfering users in a CM1 multipath channel.

It can be observed in Fig. 4 that the conventional receiver performs poorly, rapidly approaching an error floor of approximately 0.04 by 15 dB SNR. In Fig. 5 also, the bit error rate of the conventional receiver is relatively large, except when the interference is negligible. The hard-limiting receiver and the soft-limiting receiver, which apply the nonlinear transformation to each PDS before combining, show much better performance in Fig. 4 for large SNR, several orders of magnitude superior in BER to the conventional receiver. However, these nonadaptive receivers show worse performance than the conventional receiver at small SNR; here, Gaussian noise is dominant, and the conventional receiver is the optimal receiver for Gaussian noise. A similar effect is seen in Fig. 5; the receivers with fixed nonlinear transformations perform much better than the conventional receiver for most of the SIR range, but at large SNR become much worse than the conventional receiver, reflecting poorer performance in Gaussian noise.

The receiver that uses IS to select PDSs for linear combining gives BER performance equal to or better than the conventional receiver for all SNR in Fig. 4. It improves on the conventional receiver starting at an SNR of about 5 dB, with over two orders of magnitude better performance for large SNR. At moderate to large SNR, the receivers employing static nonlinear transformations have superior performance to the receiver using linear combining with IS. The receiver using the IS structure is able to avoid most but not all interference, and linear combining remains sensitive even to rare interfering pulses. In Fig. 5, again the linear IS receiver always matches or improves on the conventional receiver, and it is much better than the conventional receiver for low SIR. For example, at a BER of 10^{-2}, the IS receiver is approximately 7 dB better in SIR than the CMF receiver. The linear receivers also are much better than the static nonlinear receivers for large SIR. While the nonlinear receivers offer superior performance to the IS-based linear receiver for small SIR, the performance difference is smaller in this moderate-SNR case than for the largest values of SNR examined in Fig. 4.

The receivers employing both IS and a nonlinear operation are seen to have the best BER performance for all SNRs in the comparison of Fig. 4, improving on the static nonlinear receivers for SNRs greater than 12 dB with over one order of magnitude better BER performance at large SNR. In the moderate-SNR region, the IS signal is used to switch the nonlinear transformation per-PDS, while for larger SNR values, the IS signal is used to select transformed PDSs for combining. Superior BER performance versus SIR is observed in Fig. 5.

More complex nonlinear PDS transformation techniques have been evaluated in similar structures, and in each case improvement was observed over the underlying technique. It has also been observed that a computationally simpler hard or soft limiter used together with an IS structure can be as effective as a receiver using more complex nonlinearities such as that of [6].

VI. Conclusion

A novel MUI sensing concept has been presented together with Rake receiver designs employing MUI sensing structures. The new designs offer superior performance compared to the both the conventional receiver and compared to corresponding nonlinear receivers when MUI is significant, and no loss of performance at large SIR or small SNR. Additional designs and an expansion of these concepts can be found in [11].

References

[1] M. Z. Win and R. A. Scholtz, "Ultra-wide bandwidth time-hopping spread-spectrum impulse radio for wireless multiple-access communications," *IEEE Trans. Commun.*, vol. 48, no. 4, pp. 679–689, Apr. 2000.

[2] ——, "Impulse radio: how it works," *IEEE Commun. Lett.*, vol. 2, no. 2, pp. 36–38, Feb. 1998.

[3] N. C. Beaulieu and D. J. Young, "Designing time-hopping ultrawide bandwidth receivers for multiuser interference environments," *Proc. IEEE*, vol. 97, no. 2, pp. 255–284, Feb. 2009.

[4] N. C. Beaulieu and B. Hu, "Soft-limiting receiver structures for time-hopping UWB in multiple-access interference," *IEEE Trans. Veh. Technol.*, vol. 57, no. 2, pp. 810–818, Mar. 2008.

[5] N. C. Beaulieu and S. Niranjayan, "UWB receiver designs based on a Gaussian-Laplacian noise-plus-MAI model," *IEEE Trans. Commun.*, vol. 58, pp. 997–1006, Mar. 2010.

[6] N. C. Beaulieu, H. Shao, and J. Fiorina, "P-order metric UWB receiver structures with superior performance," *IEEE Trans. Commun.*, vol. 56, pp. 1666–1676, Oct. 2008.

[7] S. Niranjayan and N. C. Beaulieu, "A myriad filter detector for UWB multiuser communication," in *Proc. IEEE Int. Conf. Commun.*, Beijing, May 2008, pp. 3918–3922.

[8] S. Gezici, A. F. Molisch, H. Kobayashi, and H. V. Poor, "Low-complexity MMSE combining for linear impulse radio UWB receivers," in *Proc. IEEE Int. Conf. Commun.*, vol. 10, 2006, pp. 4706–4711.

[9] A. F. Molisch, "Ultra-wide-band propagation channels," *Proc. IEEE*, vol. 97, no. 2, pp. 353–371, Feb. 2009.

[10] A. F. Molisch, J. R. Foerster, and M. Pendergrass, "Channel models for ultrawideband personal area networks," *IEEE Wireless Commun. Mag.*, vol. 10, no. 6, pp. 14–21, Dec. 2003.

[11] D. J. Young, "Time-hopping ultra-wide bandwidth receivers for multiuser interference environments," Ph.D. dissertation, University of Alberta, Edmonton, AB, Canada, 2010.

[12] H. Shao and N. C. Beaulieu, "A novel zonal UWB receiver with superior performance," *IEEE Trans. Commun.*, vol. 57, pp. 1197-1206, Apr. 2009.

[13] S. Boyd and L. Vandenberghe, *Convex Optimization*. Cambridge, UK: Cambridge, 2004.